Infrared Physics & Technology 75 (2016) 65–69

Contents lists available at ScienceDirect

Infrared Physics & Technology

journal homepage: www.elsevier.com/locate/infrared

InGaAsP/InP photodetectors targeting on 1.06 μm wavelength detection

S.P. Xi [a], Y. Gu [a], Y.G. Zhang [a,*], X.Y. Chen [a], Y.J. Ma [a], L. Zhou [a], B. Du [a], X.M. Shao [b], J.X. Fang [b]

[a] State Key Laboratory of Functional Materials for Informatics, Shanghai Institute of Microsystem and Information Technology, Chinese Academy of Sciences, Shanghai 200050, China
[b] Key Laboratory of Infrared Imaging Materials and Devices, Shanghai Institute of Technical Physics, Chinese Academy of Sciences, Shanghai 200083, China

HIGHLIGHTS

- InGaAsP photodetectors targeting on 1.06 μm wavelength have been demonstrated.
- The dark current is dramatically lower than $In_{0.53}Ga_{0.47}As$ detector.
- The detectivity at 1.06 μm is much higher comparing to $In_{0.53}Ga_{0.47}As$ detector.
- The theoretical mechanisms are analyzed and compared to experimental results.

ARTICLE INFO

Article history:
Received 10 December 2015
Available online 23 January 2016

Keywords:
Photodetectors
InGaAsP
III–V semiconductors
Near infrared

ABSTRACT

InP-based InGaAsP photodetectors targeting on 1.06 μm wavelength detection have been grown by gas source molecular beam epitaxy and demonstrated. For the detector with 200 μm mesa diameter, the dark current at 10 mV reverse bias and R_0A are 8.89 pA (2.2×10^{-8} A/cm^2) and $3.9 \times 10^5\ \Omega\,cm^2$ at room temperature. The responsivity and detectivity of the InGaAsP detector are 0.30 A/W and 1.45×10^{12} cm Hz$^{1/2}$ W^{-1} at 1.06 μm wavelength. Comparing to the reference $In_{0.53}Ga_{0.47}As$ detector, the dark current of this InGaAsP detector is about 570 times lower and the detectivity is more than ten times higher, which agrees well with the theoretical estimation.

1. Introduction

In the optoelectronic applications adopting laser sources, for instance the active imaging, ranging or 3D lidar, the performances of the lasers and photodetectors (PDs) are the most important issues of concern. Among a variety of lasers the 1.06 μm solid or fiber lasers, which employs neodymium as active medium and normally pumped using mature 808 nm semiconductor lasers, should be the best one for its high efficiency and power. As for the PD materials, Si should be the most successful one but not so suitable for 1.06 μm detection because of its slightly wider and indirect band-gap. The optical absorption coefficient of Si at 1.06 μm is less than 10 cm^{-1}, which is about three orders lower than those of direct band-gap III–V materials with the same band-gap energy. Therefore, to improve the absorption of the Si PIN devices, thick absorption layers are needed and the devices are usually operated under high reverse bias to form a wide depletion region. Direct band-gap $In_{0.53}Ga_{0.47}As$ works well at 1.31 μm and 1.55 μm wavelengths and can also be used for 1.06 μm detection, but in this case its narrower band-gap results in higher dark current, also the much response out of the target wavelength is not good for the noise performance of the system. Therefore, for the target wavelength of 1.06 μm a direct band material with band-gap energy of about 1 eV is expected for the absorption layer of the PD.

Quaternary InGaAsP alloy could be lattice matched to InP substrate exactly over a range of specific compositions, and covers the band-gap energy from about 0.75 to 1.35 eV corresponding to a wide spectral range. This quaternary InGaAsP direct band material has been used widely as the active or waveguide layers of the lasers for optical communication applications as it can cover the low loss and dispersion widows of optical fibers. Notice that the band-gap energy of this quaternary could also be tailored to about 1 eV for 1.06 μm detection, so it is a promising candidate for the light absorption layer of the PD for those applications.

Some early works of liquid phase epitaxy (LPE) grown InGaAsP PIN PDs targeting on the communication wavelengths, especially 1.31 μm, have been reported [1–8]. The structural schemes, LPE growth and processing of the PDs, as well as their performances, have been reviewed in detail [8]. However, only few early works on detectors at shorter wavelength around 1.1 μm have been reported [9,10], where the structures were still grown by LPE. In this work, InGaAsP detectors targeting on the 1.06 μm wavelength detection were grown on InP substrates by gas source molecular

* Corresponding author.
E-mail address: ygzhang@mail.sim.ac.cn (Y.G. Zhang).

http://dx.doi.org/10.1016/j.infrared.2015.12.013
1350-4495/

beam epitaxy (GSMBE) system and mesa-type PD devices were fabricated. Through a comprehensive research, the characteristics of the detectors have been investigated in detail.

2. Experimental details

The detector wafers were grown on (001)-oriented InP epi-ready substrates by using a VG Semicon V90H GSMBE system. The elemental indium, gallium and aluminum were used as group III sources, and their fluxes were temperature controlled. Arsine and phosphine high-pressure cracking cells were used as group V sources. Their fluxes were controlled by adjusting the pressure. The cracking temperature was around 1000 °C, measured by thermocouple. Standard beryllium and silicon effusion cells were used as *p*-type and *n*-type doping sources, and the doping levels were also controlled by changing the temperatures. Before the growth, the fluxes of group III sources were calibrated by using an in-situ ion gauge. The lowest background pressure of this GSMBE system is less than 10^{-10} Torr, while the pressure during growth is typically in the 10^{-5} Torr range. The surface oxide desorption of the InP substrate was carried out under P_2 flux at substrate temperature around 530 °C. Before the growth of InGaAsP detector, InGaAsP single layers were grown on InP substrates to calibrate the growth parameters for lattice-matched layers. The optimal lattice mismatch between InGaAsP single layer and InP substrate was $\Delta a/a < 2 \times 10^{-4}$ measured by using X-ray diffraction measurements.

The growth of the InGaAsP PD structure began with a 1 μm N^+ InP buffer layer, then a 1.5 μm n^- InGaAsP absorbing layer and a 0.6 μm P^+ InP cap layer were grown. The final layer in the structure was a 0.15 μm P^+ $In_{0.53}Ga_{0.47}As$ contact layer. The growth rates of all the layers were around 1 μm h^{-1}.

After growth, the X-ray diffraction scan curves were measured using a Philips X'pert MRD high resolution X-ray diffractometer (HRXRD) equipped with a four-crystal Ge (220) monochromator. The photoluminescence (PL) spectra were measured using a Nicolet iS50 Fourier transform infrared spectrometer, in which a liquid-nitrogen cooled InSb detector and CaF_2 beam splitter were used.

The grown wafer was processed into mesa-type detectors with the structure shown schematically in Fig. 1. The mesa were defined by using photolithography, and then passivated by Si_3N_4 using inductively coupled plasma chemical vapor deposition. After evaporation of the contact metals and an alloy step, the wafer was diced into chips. A HP4156A semiconductor analyzer was used to perform the *I*–*V* characteristics, and a HP4280A *C*–*V* meter was used for *C*–*V* characterization.

3. Results and discussion

Fig. 2 shows the typical HRXRD ω–2θ scan curves in the (004) direction. The relatively narrower and higher peak was denoted as S corresponds to InP substrate. In order to well distinguish the epitaxial layer peaks, we removed the $In_{0.53}Ga_{0.47}As$ contact layer by using selective wet etching. Through contrastive analysis, the two epitaxy layer peaks corresponding to InGaAsP absorption layer (denoted as L1) and $In_{0.53}Ga_{0.47}As$ contact layer (denoted as L2) were assigned, respectively. The InGaAsP absorption layer shows a mismatch of -2.2×10^{-4} to the InP substrate with a full width at half maximum (FWHM) of around 53 arcseconds.

The optical quality of this detector wafer, which is correlated with the performance of the optoelectronic device in a more straightforward way, was evaluated using PL measurement, and the results are shown in Fig. 3. In this measurement, a diode pumped solid state (DPSS) laser with the wavelength of 532 nm was used as exciting source. Because of the smaller band-gap of the $In_{0.53}Ga_{0.47}As$ contact layer, almost all the incident light was absorbed by this contact layer. Only the PL signal of $In_{0.53}Ga_{0.47}As$ contact layer at about 1.67 μm is observed for the unetched sample, whereas PL signal from InGaAsP is unable to be observed. The PL spectra of the sample with InGaAs contact layer etched away is also shown in Fig. 3. A strong PL peak at around 1.25 μm could be seen at room temperature, corresponding to the InGaAsP absorption layer.

Fig. 4 shows the *C*–*V* characteristic of the detector measured at 1 MHz frequency and room temperature by using a HP4280A *C*–*V* meter. For the detector with 200 μm mesa diameter, the zero-biased capacitance is 9.38 pF (2.34×10^{-8} F/cm^2) as shown in Fig. 4. The carrier concentrations in the depletion region of the InGaAsP absorption layer educed from the *C*–*V* data are also plotted in Fig. 4. In this detector, the acceptor concentration N_A in InP layer is 3×10^{18} cm^{-3}, which is almost two orders higher than the donor concentration N_D in the InGaAsP layer. So this pn junction is a one side abrupt P^+N junction. The carrier concentration $N(x)$ in the InGaAsP absorption layer and the depletion layer width X_d were calculated by:

$$N(x) = -\frac{C^2\left(\frac{dV}{dC}\right)}{\varepsilon_r \varepsilon_0 A^2} \quad (1)$$

$$X_d = \frac{\varepsilon_r \varepsilon_0 A}{C} \quad (2)$$

where $X_d = 0$ is at the pn junction interface, ε_0 and ε_r are the dielectric constants of vacuum and InGaAsP and *A* is the area of mesa. The carrier concentration is around $1–3 \times 10^{16}$ cm^{-3}, which is consistent with the Hall data from the calibrating wafer.

Fig. 5 shows the response spectra of the detector at zero bias and room temperature, where the response has been corrected

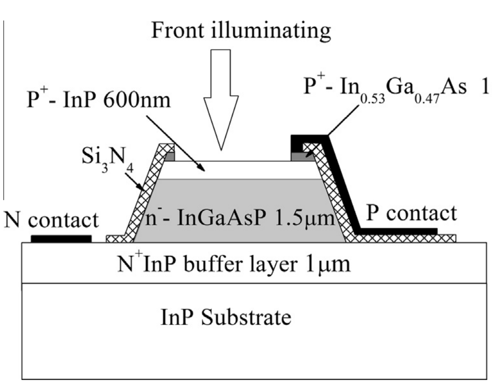

Fig. 1. The schematic of the mesa-type InGaAsP detector.

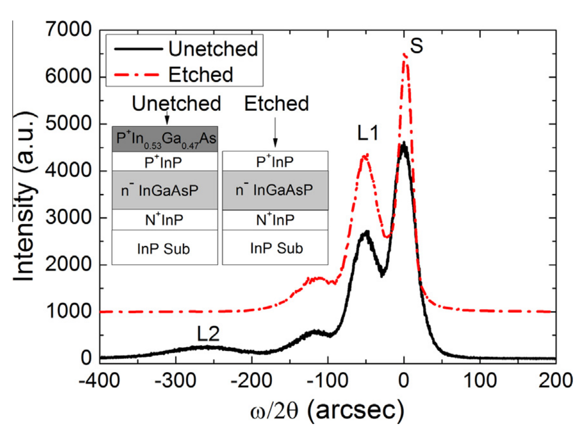

Fig. 2. (004) ω–2θ scan curves of the InGaAsP PD structures, the solid and dash lines are the unetched and etched samples respectively. The inset shows the schematic structures of the two samples.